Microbial control over host diet selection

Brian K. Trevelline[#] and Kevin D. Kohl

Department of Biological Sciences, University of Pittsburgh, Pittsburgh, Pennsylvania, 15260, USA

[#]Address correspondence to Brian K. Trevelline, brian.trevelline@gmail.com.

Abstract

Diet selection is a fundamental aspect of animal behavior with numerous ecological and evolutionary implications[1]. While the underlying mechanisms are complex, the availability of essential dietary nutrients can strongly influence diet selection[2]. The gut microbiome has been shown to metabolize many of these same nutrients[3], leading to the untested hypothesis that intestinal microbiota may influence diet selection[4,5]. Here we show that germ-free mice colonized by gut microbiota from three rodent species with distinct foraging strategies differentially selected diets that varied in macronutrient composition. Specifically, we found that herbivore-conventionalized mice voluntarily selected a higher protein:carbohydrate ratio diet, while omnivore- and carnivore-conventionalized mice selected a lower P:C ratio diet. In support of the long-standing hypothesis that tryptophan – the essential amino acid precursor of serotonin – serves as a peripheral signal regulating diet selection[6], bacterial genes involved in tryptophan metabolism and plasma tryptophan availability prior to the selection trial were significantly correlated with subsequent voluntary carbohydrate intake. Finally, herbivore-conventionalized mice exhibited larger intestinal compartments associated with microbial fermentation, broadly reflecting the intestinal morphology of their donor species. Together, these results demonstrate that gut microbiome can influence host diet selection and intestinal physiology by mediating the availability of essential amino acids, thereby revealing a novel mechanism by which the gut microbiota influence host foraging behavior.

Proper nutrition is essential to life, and thus animals have evolved complex internal sensory systems that help maintain nutritional homeostasis by regulating macronutrient intake[7]. The intestinal tract plays a critical role in this process by liberating dietary nutrients (*e.g.,* essential amino acids) that communicate the quality of a meal to central nervous system by direct stimulation of enteric nerves[8] or through post-absorptive peripheral signals[9]. The intestinal tract also harbors trillions of microorganisms (collectively known as the gut microbiome), which have been shown to influence numerous aspects of host behavior, most likely through metabolites that interact with host sensory systems[3]. Given the importance of dietary nutrients in the regulation of food intake and diet selection[2], the gut microbiome may influence host foraging behavior through metabolic processes that affect the availability of nutrients recognized by the central nervous system[4,5]. It has been suggested that gut microbiota could employ this strategy to elicit host foraging behaviors that enrich the intestinal environment in nutrients on which they depend (*i.e.,* promoting their own fitness)[4], while others have posited that a positive-feedback relationship between dietary nutrients and microbial community composition eventually results in stable microbial communities and host foraging behaviors[5]. Regardless, the notion that microbiota may affect host foraging has enormous implications for our understanding of the ecological and evolutionary processes shaping animal behavior, and possibly human health. However, these potential mechanisms operate under the assumption that the gut microbiome influences diet selection – a hypothesis that has existed for years[4,5], but has never been tested.

The transplantation of microbiota into germ-free mice is the best available approach for disentangling the effects of the gut microbiome on host behavioral phenotypes from other potentially confounding factors (*e.g.,* host genetics)[10]. To determine whether the gut microbiome influences diet selection, we chose three rodent species with distinct foraging strategies as microbial donors for germ-free mice: a carnivore/insectivore (southern grasshopper mouse, *Onychomys torridus*), an omnivore (white-footed mouse, *Peromyscus leucopus*), and an herbivore (montane vole, *Microtus montanus*). These three species are in the same taxonomic family (Cricetidae) and are all equally distantly related to lab mice (*Mus musculus*, family Muridae)[11]. Under sterile laboratory conditions, we randomly divided 30 adult male germ-free mice into Carn-CONV, Omni-CONV, and Herb-CONV treatment groups (n = 10 mice per group), where each mouse in a given group was "conventionalized" (*i.e.*, inoculated) with the cecal contents of a unique, wild-caught donor individual (to better reflect natural interindividual variation) (Fig. 1a). Conventionalized mice were acclimated to their microbiota for 7 days, during which they were offered only sterile water and a low protein:carbohydrate ratio diet (LPC; Extended Data Table 1). There were no differences in daily or cumulative macronutrient intake across treatment groups during the acclimation period (Extended Data Fig. 1; Supplemental Data 1). After acclimation, conventionalized mice were given a choice between the LPC diet and one with a higher P:C ratio (HPC; Extended Data Table 1) for a period of 11 days (Fig. 1a).

To determine whether treatment groups differed in foraging behavior, we employed a state-space approach known as the Geometric Framework for nutrition[12], which allowed us to measure the effect of the microbiome on carbohydrate and protein

intake. Supporting the hypothesis that the gut microbiome influences diet selection, this approach revealed statistically significant differences in macronutrient intake across groups of conventionalized mice (Fig. 1b). Treatment groups differed significantly in daily (Extended Data Fig. 1) and cumulative carbohydrate intake (Fig. 1b) during the diet selection trial, with Herb-CONV mice consuming fewer carbohydrates than the other groups (Fig. 1b inset). Treatment groups did not differ in either daily (Extended Data Fig. 1) or cumulative protein intake (Fig. 1b inset). Lower cumulative carbohydrate intake among Herb-CONV mice was driven by their selection of a higher P:C ratio diet compared to Omni-CONV and Carn-CONV mice (Fig. 1b). The preference of Herb-CONV mice for the HPC diet are consistent with previous studies showing that *Microtus* voles prefer high-protein foods when available[13,14], and the opportunistic consumption of high-protein meals among wild herbivores[15,16].

Next, we characterized day 0 gut microbial community structure, microbiome function, and plasma metabolites of conventionalized mice to determine how these aspects were associated with differential diet selection across treatment groups. 16S rRNA inventories confirmed that both donors and recipients harbored distinct bacterial communities, with recipients most closely resembling the communities of their donor species (Fig. 1c, Extended Data Fig. 2, Extended Data Table 2). Bacterial ASV richness and phylogenetic diversity were similar between Carn-CONV and Omni-CONV mice, but significantly lower in Herb-CONV mice (Extended Data Fig. 3). The bacterial communities of conventionalized mice were dominated by the phyla Bacteroidetes and Firmicutes (Extended Fig. 4a), with differences in the microbiome community structure across treatment groups being driven by 13 bacterial families in the phyla

Bacteroidetes, Firmicutes, and Actinobacteria (Extended Data Fig. 4b, c). Metagenomic analysis of recipient fecal samples revealed a statistically significant effect of donor species on the relative abundances of 176 (49%) KEGG functional modules (Fig. 1d; Supplemental Data 2). These differences in microbiome community structure and function were accompanied by concomitant differences in plasma metabolites (Fig. 1e), with 24 identified metabolites (14%) differing significantly across treatment groups (Supplemental Data 3). Together, these results demonstrate that interspecific differences in gut microbial communities across rodents with divergent foraging strategies translate to distinct microbial functions and metabolite profiles independent of host diet.

There is substantial evidence that the availability of circulating essential amino acids (EAAs) provide peripheral signals that act to regulate macronutrient intake and diet selection[9]. Despite consuming identical diets prior to the selection trial, treatment groups differed in circulating levels of several amino acids, with Herb-CONV mice exhibiting significantly higher amounts of the EAAs isoleucine and tryptophan (Fig. 2a), though tryptophan was only significant after the removal of two exceptionally-low statistical outliers (>1.5 x IQR) from the Herb-CONV group. While EAAs are primarily derived from the diet, bacteria can also produce these peptides through their own metabolic processes[17], and thus the gut microbiome may act as a source of EAAs for their hosts. In support of this hypothesis, treatment groups exhibited broad differences in the microbial synthesis and degradation of EAAs (Fig. 2b). Notably, the microbiome of Herb-CONV mice had a higher abundance of genes involved in the synthesis of aromatic amino acids (phenylalanine, tryptophan, and tyrosine) (Fig. 2b), all of which

are synthesized from chorismate (product of the Shikimate pathway)[18]. The ratios of bacterial genes involved in tryptophan biosynthesis (M00023) to those involved in tryptophan degradation via the kynurenine pathway (M00038) were significantly correlated with plasma tryptophan (Fig. 2c). Given that conventionalized mice consumed identical diets prior to blood collections, these results demonstrate that bacterial metabolism can alter the availability of circulating levels of plasma EAAs.

There is emerging evidence that bacterial tryptophan metabolism is a key mechanism by which the gut microbiome can influence host behavior[19,20]. This relationship is a consequence of tryptophan's role as the primary regulatory molecule for the synthesis of central serotonin (5-hydroxytryptamine, 5-HT)[21], which has been shown to drive foraging behavior and diet selection in several experimental studies[6]. For example, when given a choice between low- or high-carbohydrate meals, rats receiving hypothalamic injections of 5-HT significantly reduced their carbohydrate intake[22]. Importantly, serotonin synthesis is extraordinarily sensitive to plasma tryptophan availability, and thus plasma tryptophan is generally considered a reliable proxy for central serotonin[23]. Therefore, we predicted that plasma tryptophan would be associated with differences in diet selection among conventionalized mice. Indeed, we found a statistically significant correlation between day 0 plasma tryptophan and subsequent voluntary carbohydrate and P:C intake (Fig. 2c). More recent work has argued that serotonin synthesis is affected by the availability of tryptophan relative to the large neutral amino acids (LNAA: Leu, Ile, Phe, Tyr, and Val) that compete for transport across the blood brain barrier[24]. Consistent with these studies, we found a statistically significant correlation between day 0 Trp:LNAA ratios, cumulative

carbohydrate intake, and P:C intake (Fig. 2c). Further, the ratio of tryptophan biosynthesis and degradation modules were also statistically significant predictors of carbohydrate and P:C intake (Fig. 2c). Overall, these results strongly support the hypothesis that bacterial tryptophan metabolism influences host diet selection.

Interspecific differences in foraging behavior are generally associated with diet-specific adaptations to intestinal physiology. For example, herbivores generally maintain an enlarged cecum (fermentation chamber) that enhances the digestibility of low-quality, carbohydrate-rich foods[25]. Given that the gut microbiome can profoundly alter host intestinal gene expression and physiology[26-28], divergent microbial communities may drive differences in intestinal morphology across feeding strategies. At the conclusion of the diet selection trial (day 11), we quantified intestinal morphology with the prediction that conventionalized mice would exhibit differences that broadly reflected that of their donor species. Consistent with evolutionary adaptations to herbivory, treatment groups differed significantly in empty cecum mass (Fig. 3a), empty colon mass (Fig. 3b), and colon length (after the removal of an exceptionally-high statistical outlier from the Carn-CONV group) (Fig. 3c), with comparatively larger intestinal compartments among the Herb-CONV mice. There was no change in body mass over the duration of the experiment ($F = 1.66$, $P = 0.327$). The obvious question is whether the gut microbiome affected intestinal morphology directly or via differential diet selection. While our experimental design makes it difficult to disentangle the effects of differential diet selection from those of microbiome, it is worth noting that previous work has demonstrated that lab mice fed low P:C ratio diets had larger intestinal compartments (*e.g.,* cecum and colon) compared to those fed higher P:C diets[28]. In our study, we

observed the opposite – Herb-CONV mice, which consumed a higher P:C ratio diet (Fig. 1b), exhibited larger cecum and colon masses (Fig. 3). These results contradict the generally accepted model of adaptive physiological responses to dietary carbohydrates, suggesting that the gut microbiome may drive interspecific differences in host intestinal physiology independent from those of diet and genetics.

The gut microbiome is now recognized as a key player in host digestion, performance, and health[29], leading to the realization that animals should no longer be thought of as singular entities, but rather as 'holobionts' – complex genetic and biomolecular networks composed of the host plus its associated microbiota, upon which natural selection acts[30]. In support of these concepts, our study provides the first evidence that variation in the gut microbiome can influence diet selection, which is a fundamental aspect of host behavior. Specifically, we showed that host species-associated gut microbiota can produce statistically significant differences in the diet selection of conventionalized mice in just 11 days, likely through differential bacterial metabolism and downstream availability of EAAs, especially tryptophan. These findings provide evidence of a mechanistic link between the gut microbiome and animal behavior, with implications for large-scale evolutionary processes involving diet, nutrition, and foraging ecology.

REFERENCES

1 Stephens, D. W., Brown, J. S. & Ydenberg, R. C. *Foraging: behavior and ecology*. (University of Chicago Press, 2008).

2 Berthoud, H. R., Münzberg, H., Richards, B. K. & Morrison, C. D. Neural and metabolic regulation of macronutrient intake and selection. *Proceedings of the Nutrition Society* **71**, 390-400 (2012).

3 Cryan, J. F. *et al.* The microbiota-gut-brain axis. *Physiological Reviews* **99**, 1877-2013 (2019).

4 Alcock, J., Maley, C. C. & Aktipis, C. A. Is eating behavior manipulated by the gastrointestinal microbiota? Evolutionary pressures and potential mechanisms. *BioEssays* **36**, 940-949 (2014).

5 Norris, V., Molina, F. & Gewirtz, A. T. Hypothesis: bacteria control host appetites. *Journal of Bacteriology* **195**, 411-416 (2013).

6 Blundell, J. E. & Halford, J. C. Serotonin and appetite regulation. *CNS Drugs* **9**, 473-495 (1998).

7 Kyriazakis, I., Tolkamp, B. J. & Emmans, G. Diet selection and animal state: an integrative framework. *Proceedings of the Nutrition Society* **58**, 765-772 (1999).

8 Furness, J. B. The enteric nervous system and neurogastroenterology. *Nature Reviews Gastroenterology & Hepatology* **9**, 286 (2012).

9 Stubbs, R. J. Peripheral signals affecting food intake. *Nutrition* **15**, 614-625 (1999).

10 Luczynski, P. *et al.* Growing up in a bubble: using germ-free animals to assess the influence of the gut microbiota on brain and behavior. *International Journal of Neuropsychopharmacology* **19** (2016).

11 Steppan, S. J., Adkins, R. M. & Anderson, J. Phylogeny and divergence-date estimates of rapid radiations in muroid rodents based on multiple nuclear genes. *Systematic Biology* **53**, 533-553 (2004).

12 Simpson, S. J. & Raubenheimer, D. A multi-level analysis of feeding behaviour: the geometry of nutritional decisions. *Philosophical Transactions of the Royal Society of London. Series B: Biological Sciences* **342**, 381-402 (1993).

13 Harju, A. & Hakkarainen, O. Effect of protein and birch-bark powder on selection of food by root voles (*Microtus oeconomus*). *Journal of Mammalogy* **78**, 563-568 (1997).

14 Bergeron, J. & Jodoin, L. Defining “high quality” food resources of herbivores: the case for meadow voles (*Microtus pennsylvanicus*). *Oecologia* **71**, 510-517 (1987).

15 Nie, Y. *et al.* Giant pandas are macronutritional carnivores. *Current Biology* **29**, 1677-1682. e1672 (2019).

16 Ulappa, A. C. *et al.* Plant protein and secondary metabolites influence diet selection in a mammalian specialist herbivore. *Journal of Mammalogy* **95**, 834-842 (2014).

17 Dai, Z. L., Wu, G. & Zhu, W. Y. Amino acid metabolism in intestinal bacteria: links between gut ecology and host health. *Frontiers in Bioscience* **16**, 1768-1786 (2011).

18 Herrmann, K. M. & Weaver, L. M. The shikimate pathway. *Annual Review of Plant Biology* **50**, 473-503 (1999).

19 Gao, K., Mu, C. L., Farzi, A. & Zhu, W. Y. Tryptophan metabolism: a link between the gut microbiota and brain. *Advances in Nutrition* (2019).

20 O'Mahony, S. M., Clarke, G., Borre, Y., Dinan, T. & Cryan, J. Serotonin, tryptophan metabolism and the brain-gut-microbiome axis. *Behavioural Brain Research* **277**, 32-48 (2015).

21 Fernstrom, J. D. Role of precursor availability in control of monoamine biosynthesis in brain. *Physiological Reviews* **63**, 484-546 (1983).

22 Shor-Posner, G., Grinker, J. A., Marinescu, C., Brown, O. & Leibowitz, S. F. Hypothalamic serotonin in the control of meal patterns and macronutrient selection. *Brain Research Bulletin* **17**, 663-671 (1986).

23 Fernstrom, J. D. & Wurtman, R. Brain serotonin content: physiological dependence on plasma tryptophan levels. *Science* **173**, 149-152 (1971).

24 Fernstrom, J. D. Large neutral amino acids: dietary effects on brain neurochemistry and function. *Amino Acids* **45**, 419-430 (2013).

25 Stevens, C. E. & Hume, I. D. *Comparative physiology of the vertebrate digestive system*. (Cambridge University Press, 2004).

26 Chevalier, C. *et al.* Gut microbiota orchestrates energy homeostasis during cold. *Cell* **163**, 1360-1374 (2015).

27 Broderick, N. A., Buchon, N. & Lemaitre, B. Microbiota-induced changes in Drosophila melanogaster host gene expression and gut morphology. *MBio* **5**, e01117-01114 (2014).

28 Sørensen, A., Mayntz, D., Simpson, S. J. & Raubenheimer, D. Dietary ratio of protein to carbohydrate induces plastic responses in the gastrointestinal tract of mice. *Journal of Comparative Physiology B* **180**, 259-266 (2010).

29 McFall-Ngai, M. *et al.* Animals in a bacterial world, a new imperative for the life sciences. *Proceedings of the National Academy of Sciences* **110**, 3229-3236 (2013).

30 Bordenstein, S. R. & Theis, K. R. Host biology in light of the microbiome: ten principles of holobionts and hologenomes. *PLoS Biology* **13**, e1002226 (2015).

FIGURES

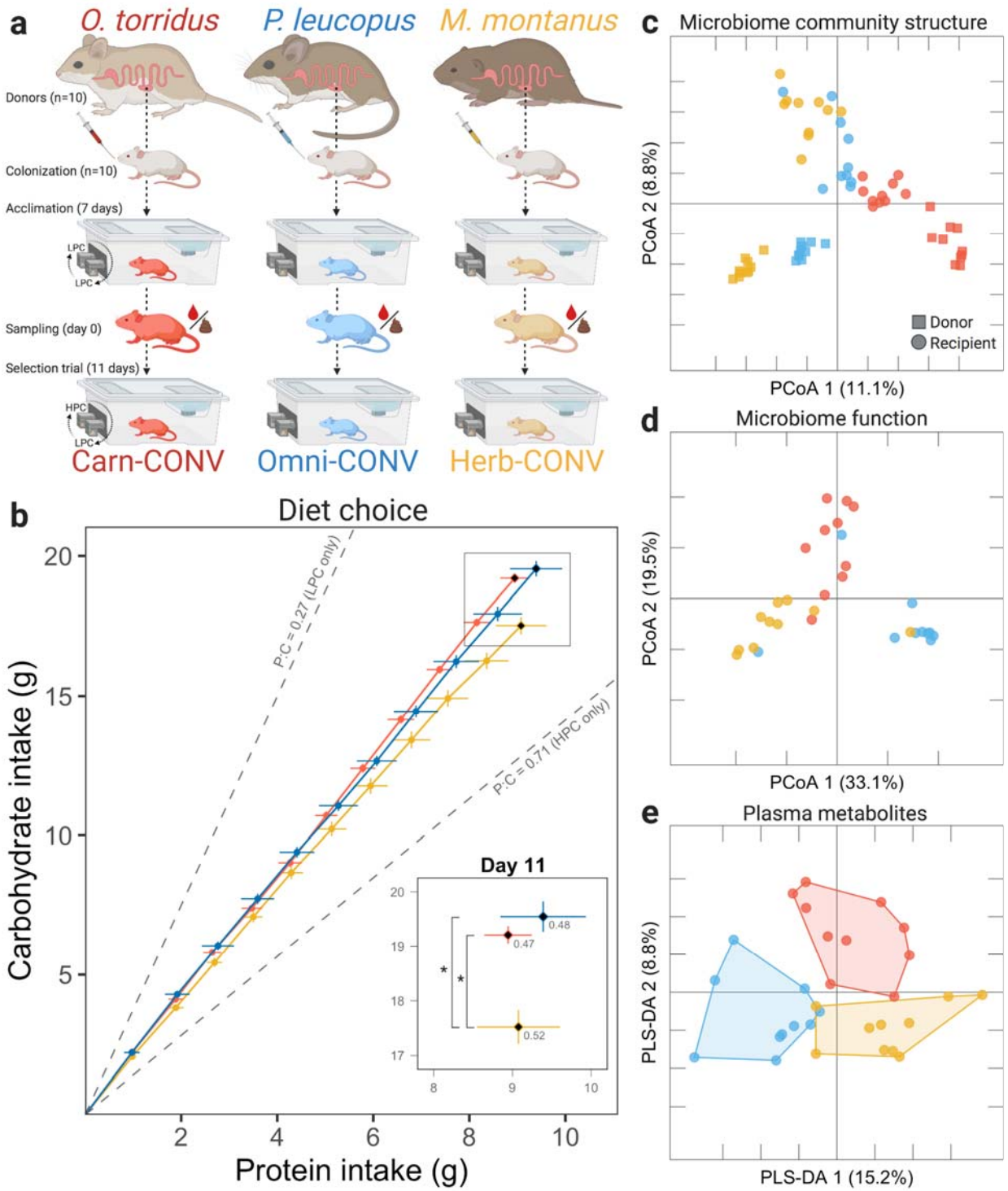

Fig. 1. The gut microbiome influences host diet selection. a, Overview of experimental design. Germ-free mice were colonized with the gut microbiome of three

species of wild rodents with distinct foraging strategies: carnivorous *Onychomys torridus* (Carn-CONV), omnivorous *Peromyscus leucopus* (Omni-CONV), and herbivorous *Microtus montanus* (Herb-CONV). Conventionalized mice were acclimated on LPC diet for 7 days before day 0 blood and fecal sampling. Conventionalized mice were then given a choice between LPC and HPC diets for 11 days. Daily diet intakes were tracked via two feeder hoods, which were rotated daily to avoid learned preferences. **b,** Treatment groups differed significantly in macronutrient intake (Wilks' λ = 0.67, P = 0.037), with Herb-CONV mice voluntarily consuming fewer carbohydrates than the Omni- and Carn-CONV groups (F = 5.42, P = 0.011). There was no difference in cumulative protein intake across treatment groups (F = 0.72, P = 0.497). Dashed rails and associated P:C ratios indicate the expected result if mice consumed only a single diet, while P:C ratios next to the cumulative macronutrient intake points for each treatment group indicates observed P:C ratio intake. **c,** Principal coordinate analysis (PCoA) of 16S rRNA inventories of wild donors (squares) and conventionalized recipients at day 0 (circles) using Bray-Curtis dissimilarity. Microbial community structure differed significantly among wild donors (Pseudo-F = 8.45, P = 0.001) and recipients (Pseudo-F = 3.55, P = 0.001), with recipients most closely resembling the communities of their donor species (Extended Data Table 2). **d,** PCoA analysis showing a statistically significant difference in the relative abundances of microbial KEGG modules using Bray-Curtis dissimilarity (Pseudo-F = 6.48, P = 0.001). **e,** PLS-DA analysis illustrating broad differences in identified plasma metabolites across conventionalized mice at day 0 (R^2 = 0.92, Q^2 = 0.30). * denotes P ≤ 0.05.

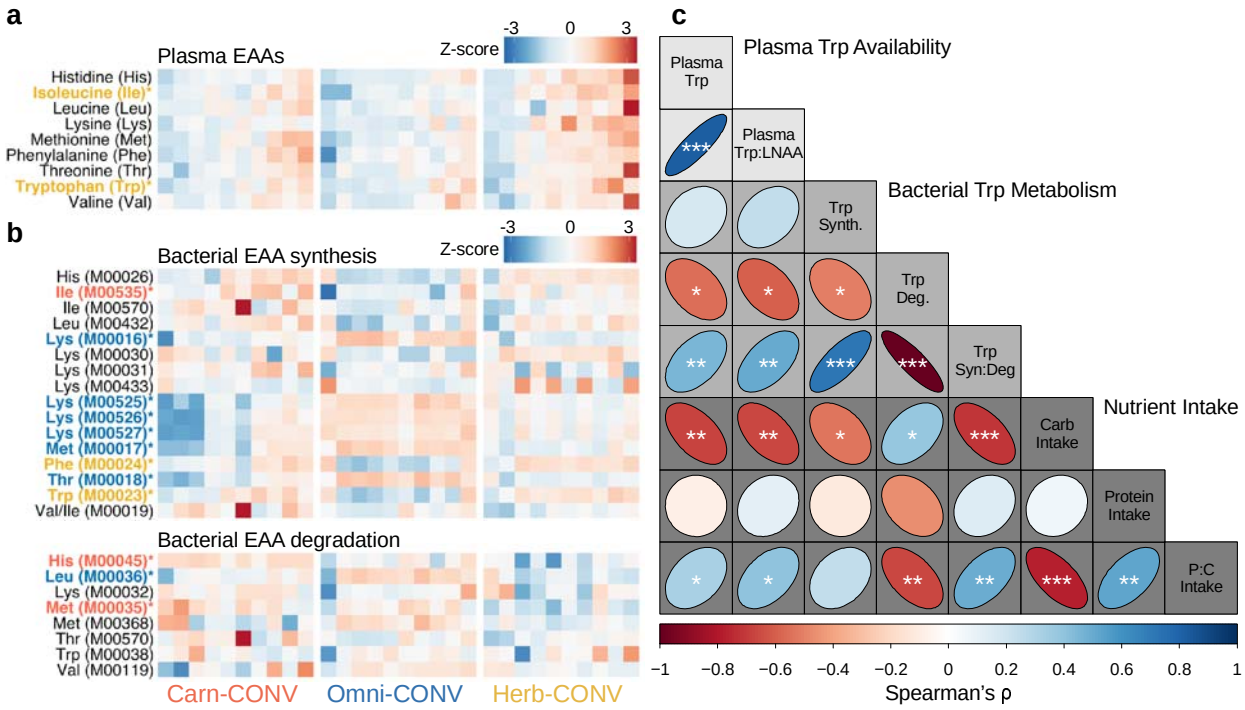

Fig. 2. Day 0 plasma tryptophan availability and bacterial tryptophan metabolism are associated with differential macronutrient intake across treatment groups. a, Heatmap illustrating broad differences in plasma levels of essential amino acids across treatment groups, with Herb-CONV mice exhibiting significantly greater levels of isoleucine (X^2 = 7.95, P = 0.019) and tryptophan (X^2 = 7.12, P = 0.029). Columns represent individual conventionalized mice for each treatment group. * denotes P ≤ 0.05 and color indicates the treatment group with greatest circulating plasma levels (red = Carn-CONV, blue = Omni-CONV, and yellow = Herb-CONV). **b,** Heatmap illustrating broad differences in the abundances of microbial genes associated with metabolism of essential amino acids (Supplemental Data 3). * denotes P ≤ 0.05 and color indicates the treatment group with greatest relative abundance. **c,** Correlation plot summarizing relationships between plasma tryptophan availability, bacterial tryptophan metabolism, and host diet selection among conventionalized mice. The direction and color of the

ellipses indicate whether correlations were positive or negative, and asterisks indicate whether Spearman's correlations were statistically significant (* denotes $P \leq 0.05$, ** denotes $P < 0.01$, and *** denotes $P < 0.001$).

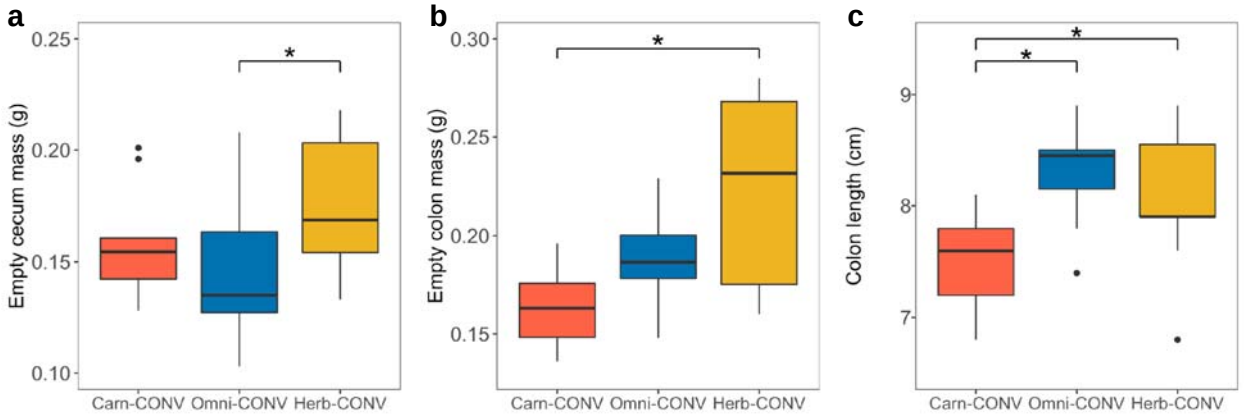

Fig. 3. Treatment groups exhibit differences in intestinal morphology that broadly reflect that of their donor species. a, Empty cecum mass differed significantly across treatment groups (F = 4.19, P = 0.027), with Herb-CONV mice exhibiting a greater cecum mass than Omni-CONV mice. **b,** Empty colon mass differed significantly across treatment groups (F = 6.65, P = 0.005; Fig. 3b), with Herb-CONV mice exhibiting a greater colon mass than Carn-CONV mice. **c,** Colon length differed significantly across treatment groups (F = 7.30, P = 0.003), with Carn-CONV mice exhibiting shorter colons compared to Omni- and Herb-CONV mice**.** * denotes P ≤ 0.05.

METHODS

Wild rodents. Wild *Onychomys torridus* were collected in August 2018 from field sites in near Green Valley, Pima Co., AZ (31.802834, -110.891172), *Peromyscus leucopus* in May 2018 near Murray, Calloway Co., KY (36.686582, -88.221204), and *Microtus montanus* in July 2018 at Timpie Springs Waterfowl Management Area, Dugway, Tooele Co., UT (40.753708, -112.639903). Ten individuals from each species were collected using baited Sherman live traps under the following state permits: *O. torridus* (AZ Game and Fish Dept., SP627958), *P. leucopus* (KY Dept. of Fish and Wildlife, SC1911097), and *M. montanus* (UT Division of Wildlife Resources, 1COLL5194-2). Animals were euthanized within 12 hours and immediately dissected under IACUC protocols registered at the University of Utah (16-02011 to D. Dearing), Murray State University (2018-026 to T. Derting), and University of Alabama (18-04-1159 to S. Secor). Cecum contents for microbiome transplants were transferred using to 1.7 mL Eppendorf tube using sterile instruments and immediately frozen at -20ºC.

Microbiome transplants. Donor cecum contents were diluted at 100mg/mL in sterile phosphate-buffered saline containing 0.2 g/L Na_2S and 0.5 g/L cysteine as reducing agents[31,32]. Under sterile laboratory conditions, 30 adult (aged 6-8 weeks) male germ-free C57BL/6 mice (Taconic Biosciences, Inc., Rensselaer, NY) were randomly divided into Carn-CONV, Omni-CONV, and Herb-CONV groups where each mouse in a given group was colonized by oral gavage of 200 µL of fecal slurry from a unique, wild-caught donor individual. Conventionalized mice were then singly-housed in sterile static cages (Innovive, Inc., San Diego, CA; MSX2-AD) modified by the addition of two metabolic feeder hoods (Laboratory Products, Inc., Seaford, DE; 2110S) that

prevent mice from caching powdered diets, and thus enable the tracking daily macronutrient intake (see below).

Diet selection experiment. After colonization, conventionalized mice were acclimated for 7 days (to allow the gut microbiome to stabilize[32]), during which they were offered only sterile water and a low protein:carbohydrate ratio diet (LPC [0.27]; Extended Data Table 1). After acclimation (day 0), mice were briefly removed from their cages for a 200 µL blood draw for metabolomics analysis (see details below). Mice were weighed (rounded to nearest hundredth) and returned to empty cages to facilitate the collection of fresh fecal samples for 16S rRNA microbial inventories and shotgun metagenomics (see details below). Conventionalized mice were then presented with a choice between two isocaloric diets (Extended Data Table 1): (1) the LPC (0.27) diet offered during acclimation and (2) a diet with a higher P:C ratio (HPC [0.71]). The positions of these two diets were rotated daily to avoid learned preferences. Diets were designed by Teklad/Envigo (Indianapolis, IN), and were powdered prior sterilization to be visually indistinguishable from each other and to prevent food caching. Daily food consumption was calculated as the difference between the mass (rounded to nearest thousandth) of each diet presented (~8 g) and the mass of each diet remaining after a 24-hour period. After tracking diet preferences for 11 consecutive days, animals were euthanized and dissected to investigate differences in the empty masses (rounded to nearest thousandth) of intestinal compartments. Conventionalized mice were maintained on a 12:12-h light:dark cycle, with 21°C ambient temperature and 40% humidity for the duration of the experiment. Animal experiments were conducted at the

University of Pittsburgh Plum Borough Primate Facility under IACUC protocol 19074445.

Metabolomics. Blood plasma was analyzed for primary metabolites (amino acids, hydroxyl acids, carbohydrates, sugar acids, sterols, aromatics, nucleosides, amines, and miscellaneous compounds) by the West Coast Metabolomics Center at the University of California – Davis, which performed all sample preparation, data acquisition, and data processing as previously described[33]. Briefly, metabolites were extracted using a mixture of acetonitrile:isopropanol:water (3:3:2, v/v/v) as well as 1:1 acetonitrile:water for removal of protein from serum. Dried metabolite extracts were resuspended in methoxyamine hydrochloride in pyridine for derivatization before being analyzed using gas chromatography-time-of-flight (GC-TOF) using a LECO Pegasus IV mass spectrometer equipped with automated liner exchange (ALEX; Gerstel corporation) and cold injection system (CIS; Gerstel corporation) for data acquisition. The CIS temperature was set at 50 °C to 250 °C final temperature at a rate of 12 °C s−1. Raw GC-TOF MS data were preprocessed with ChromaTOF (version 2.32) and apex masses were used to identify metabolites using the BinBase database. Values were reported as peak height for the quantification ion (*m/z* value) at the specific retention index, which is more precise than peak area for low abundant metabolites. All database entries that were positively detected in more than 10% of the samples of a study design class for unidentified metabolites were reported. Raw peak heights were vector normalized to reduce the impact of between-series drifts of instrument sensitivity, caused by machine maintenance status and tuning parameters.

DNA extractions. DNA was extracted from donor cecal contents and day 0 conventionalized mouse feces using the Qiagen PowerFecal DNA Kit (Qiagen, Hilden, Germany; 12830) following the manufacturer's instructions.

16S rRNA microbial inventories. Extracted DNA from conventionalized mice and donor cecum contents was amplified and sequenced by the Genome Research Core of the University of Illinois at Chicago as previously described[34]. Briefly, polymerase chain reaction (PCR) was used to amplify a portion of the bacterial 16S rRNA gene for Illumina sequencing using the Earth Microbiome Project primers 515F (GTGCCAGCMGCCGCGGTAA) and 806R (GGACTACNVGGGTWTCTAAT) targeting the V4 region of microbial small subunit ribosomal RNA gene[35]. Amplicon libraries were sequenced using a 2x251 paired-end run on an Illumina MiSeq. Raw Illumina sequencing reads (1,977,423) were paired and quality filtered via the DADA2 pipeline[36] in QIIME2 (version 2020.2)[37] using default parameters. Sequences that passed the quality filter were clustered into amplicon sequence variants (ASVs), which were identified using the SILVA reference database (release 132)[38]. Identified ASVs were filtered to exclude non-bacterial sequences (archaea, chloroplast, eukaryote, and mitochondria), reducing our total number of reads to 1,423,306 (mean of 23,722 per sample ± 7,560 SD) and 4,282 ASVs. We rarefied ASV tables to the sample with fewest number of reads (4,174) before comparisons of alpha (ASV richness and Faith's phylogenetic diversity) and beta diversity (Bray-Curtis and unweighted/weighted UniFrac distances[39]).

Shotgun metagenomics. Extracted DNA from conventionalized mice was sent to CoreBiome, Inc. (St. Paul, MN) for shotgun metagenomic analysis using

BoosterShot™ . Briefly, sequencing libraries were prepared using a procedure adapted from the Illumina Nextera Library Prep Kit (Illumina, 20018705) and sequenced on an Illumina NovaSeq using single-end 1x100 reads with the Illumina NovaSeq SP reagent kit (Illumina, 20027464). Raw sequences (125,629,570) were filtered for low quality (Q-Score < 30) and length (< 50), trimmed of adapter sequences, and converted into a single fasta using shi7 (version 0.99)[40]. Sequences were then trimmed to a maximum length of 100 bp and aligned using BURST (version 0.99.8)[41] at 97% identity against CoreBiome's Venti database consisting of all RefSeq bacterial genomes with additional manually curated strains as well as a bacterial KEGG[42] annotated database created from de-replicating the bacterial genes within the Venti database. KEGG orthology counts were converted to relative abundance within a sample and collapsed into KEGG modules for statistical analysis.

Statistics. Differences in macronutrient intake across treatment groups were tested using a repeated-measures multivariate analysis of variance (MANOVA) while controlling for the effects of body mass and donor species. Microbial community structure (from 16S rRNA inventories) was visualized using principal coordinates analysis (PCoA) on ASV relative abundances, which were then assessed for differences (controlling for multiple comparisons using false discovery rate corrected P-values) across treatment groups using non-parametric permutational multivariate analysis of variance (PERMANOVA), analysis of similarity (ANOSIM), and permutational analysis of dispersion (PERMDISP) in QIIME2[37]. Microbiome function (from metagenomics) was visualized using PCoA on KEGG module relative abundances and analyzed for differences across treatment groups with PERMANOVA in QIIME2. Differences in the

relative abundance of bacterial phyla and genera, and functional KEGG modules across conventionalized mice were tested using the non-parametric Krustal-Wallis test and linear discriminant analysis in LEfSe using the "one-against-all" strategy for multi-class analysis[43]. Identified plasma metabolites were filtered (based on mean intensity and IQR) and auto-scaled before using non-parametric ANOVAs to identify metabolites that varied significantly across treatment groups and visualized using supervised partial least square discriminant analysis (PLS-DA) in MetaboAnalyst (version 4.0)[44]. Non-parametric Spearman rank correlations between plasma Trp availability, Trp KEGG modules, and macronutrient intake were conducted using non-parametric Spearman's test (controlling for the effect of donor species) in the R package *ppcor* (version 1.1)[45] and visualized using *corrplot* (version 0.85)[46]. Differences in empty cecum/colon masses and colon length across treatment groups were tested using ANOVA with body mass as a covariate and corrected for multiple comparisons using Tukey's HSD. Unless otherwise noted, all statistical tests were two-sided and conducted in JMP Pro version 14.1.0 (SAS Institute Inc., Cary, NC). For all statistical analyses, P-values ≤ 0.05 were defined as 'significant'.

METHODS REFERENCES

31 Tremaroli, V. *et al.* Roux-en-Y gastric bypass and vertical banded gastroplasty induce long-term changes on the human gut microbiome contributing to fat mass regulation. *Cell Metabolism* **22**, 228-238 (2015).

32 Molinaro, A. *et al.* Host–microbiota interaction induces bi-phasic inflammation and glucose intolerance in mice. *Molecular Metabolism* **6**, 1371-1380 (2017).

33 Fiehn, O. *et al.* Quality control for plant metabolomics: reporting MSI-compliant studies. *The Plant Journal* **53**, 691-704 (2008).

34 Trevelline, B. K., MacLeod, K. J., Langkilde, T. & Kohl, K. D. Gestation alters the gut microbiota of an oviparous lizard. *FEMS Microbiology Ecology* **95**, fiz086 (2019).

35 Caporaso, J. G. *et al.* Global patterns of 16S rRNA diversity at a depth of millions of sequences per sample. *Proceedings of the National Academy of Sciences* **108**, 4516-4522 (2011).

36 Callahan, B. J. *et al.* High-resolution sample inference from Illumina amplicon data. *Nature Methods* **13**, 581–583 (2016).

37 Bolyen, E. *et al.* Reproducible, interactive, scalable and extensible microbiome data science using QIIME 2. *Nature Biotechnology* **37**, 852-857 (2019).

38 Quast, C. *et al.* The SILVA ribosomal RNA gene database project: improved data processing and web-based tools. *Nucleic Acids Research* **41**, D590-D596 (2012).

39 Lozupone, C. & Knight, R. UniFrac: a new phylogenetic method for comparing microbial communities. *Applied and Environmental Microbiology* **71**, 8228-8235 (2005).

40 Al-Ghalith, G. A., Hillmann, B., Ang, K., Shields-Cutler, R. & Knights, D. SHI7 is a self-learning pipeline for multipurpose short-read DNA quality control. *MSystems* **3**, e00202-00217 (2018).

41 Al-Ghalith, G. & Knights, D. BURST enables optimal exhaustive DNA alignment for big data. *doi.org/10.5281/zenodo.806850* (2017).

42 Kanehisa, M. & Goto, S. KEGG: Kyoto encyclopedia of genes and genomes. *Nucleic Acids Research* **28**, 27-30 (2000).

43 Segata, N. *et al.* Metagenomic biomarker discovery and explanation. *Genome Biology* **12**, R60 (2011).

44 Chong, J., Wishart, D. S. & Xia, J. Using metaboanalyst 4.0 for comprehensive and integrative metabolomics data analysis. *Current Protocols in Bioinformatics* **68**, e86 (2019).

45 Kim, S. ppcor: partial and semi-partial (part) correlation (version 1.1). *Available from https://CRAN.R-project.org/package=ppcor* (2015).

46 Wei, T. & Simko, V. R package "corrplot": visualization of a correlation matrix (version 0.84) *Available from https://github.com/taiyun/corrplot* (2017).

Acknowledgements. This work was supported by the National Science Foundation (IOS-1942587 to K. Kohl) and a grant from the University of Pittsburgh Central Research Development Fund. We thank A. Darracq, M. D. Dearing, T. Derting, R. Martínez-Mota, and S. Secor for help with animal collections and dissections.

Author Contributions. K.D.K conceived the project. B.K.T designed the experiments, performed the experiments, collected data, interpreted the results, and wrote the manuscript with guidance from K.D.K.

Additional Information. Supplementary information is available for this paper. Sequencing data are deposited in the NCBI SRA database under PRJNA629007. The

authors declare no competing financial interests. Correspondence and requests for materials should be addressed to B.K.T. (brian.trevelline@gmail.com).

EXTENDED DATA FIGURES AND TABLES

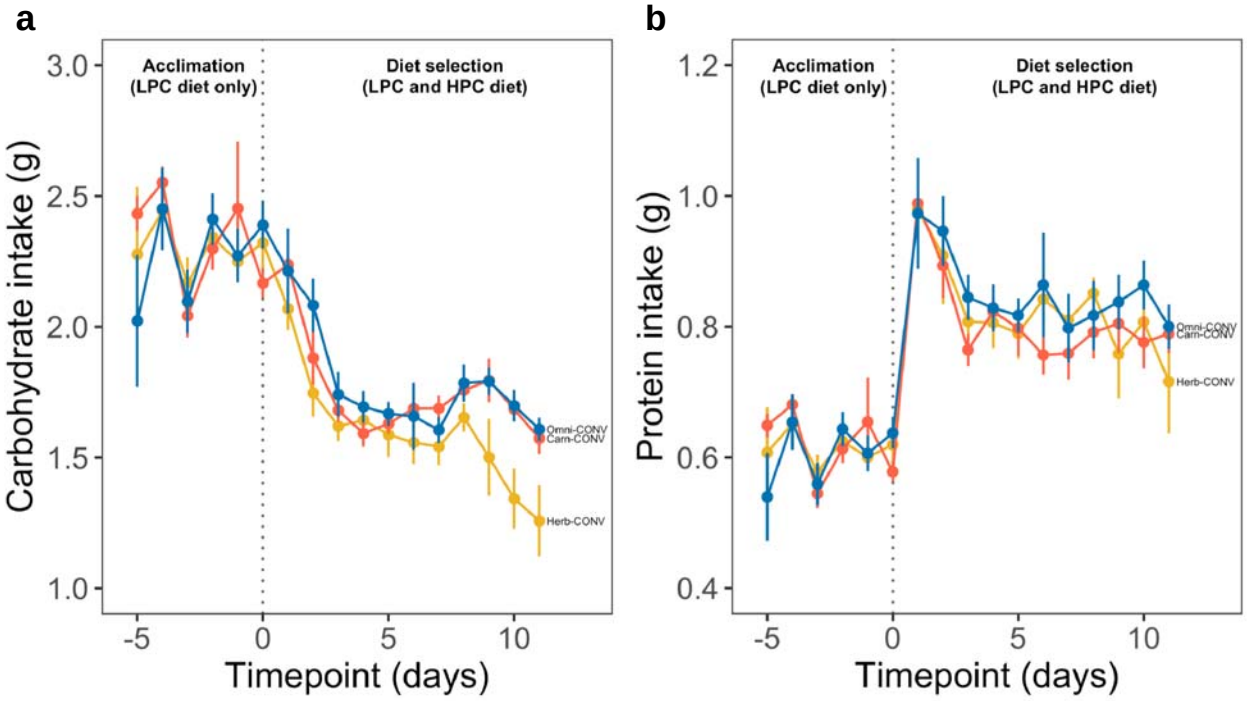

Extended Data Fig. 1. Daily macronutrient intake across treatment groups. a, Daily carbohydrate intake. During the acclimation period, there was no difference in either daily (F = 1.14, P = 0.335) or cumulative carbohydrate intake (F = 0.74, P = 0.483) across treatment groups. In contrast, there was a significant difference in daily carbohydrate intake during the diet selection experiment (F = 5.42, P = 0.011). **b,** Daily protein intake. There was no difference in daily (MANOVA, F = 1.14, P = 0.335) or cumulative protein intake (F = 0.74, P = 0.483) during the acclimation period, nor was there a difference in protein intake during the diet selection experiment (F = 0.71, P = 0.497). Line color corresponds to treatment groups: Carn-CONV (red), Omni-CONV (blue), Herb-CONV (yellow).

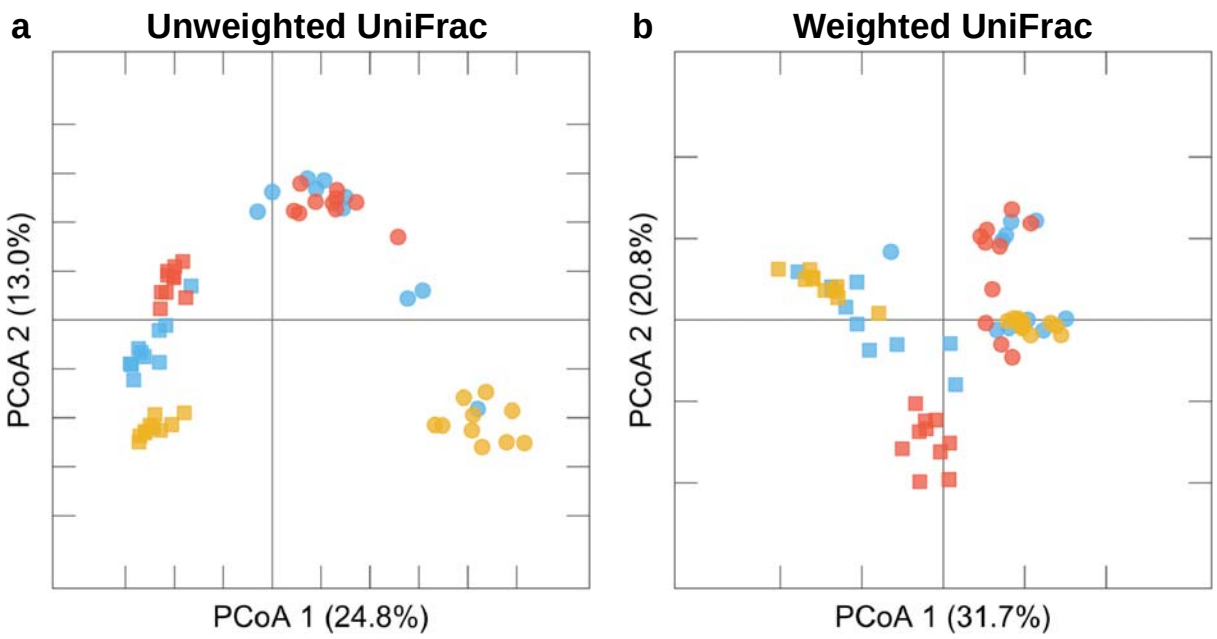

Extended Data Fig. 2. PCoA analysis of 16S rRNA inventories using unweighted and weighted UniFrac metrics. a, Principal coordinate analysis (PCoA) of unweighted UniFrac dissimilarities showing significant differences among wild donors (squares; Pseudo-F = 7.94, P = 0.001) and conventionalized mice at day 0 (circles; Pseudo-F = 6.33, P = 0.001). **b,** PCoA analysis of weighted UniFrac dissimilarities showing significant differences among wild donors (squares; Pseudo-F = 14.73, P = 0.001) and conventionalized mice at day 0 (circles; Pseudo-F = 7.35, P = 0.001).

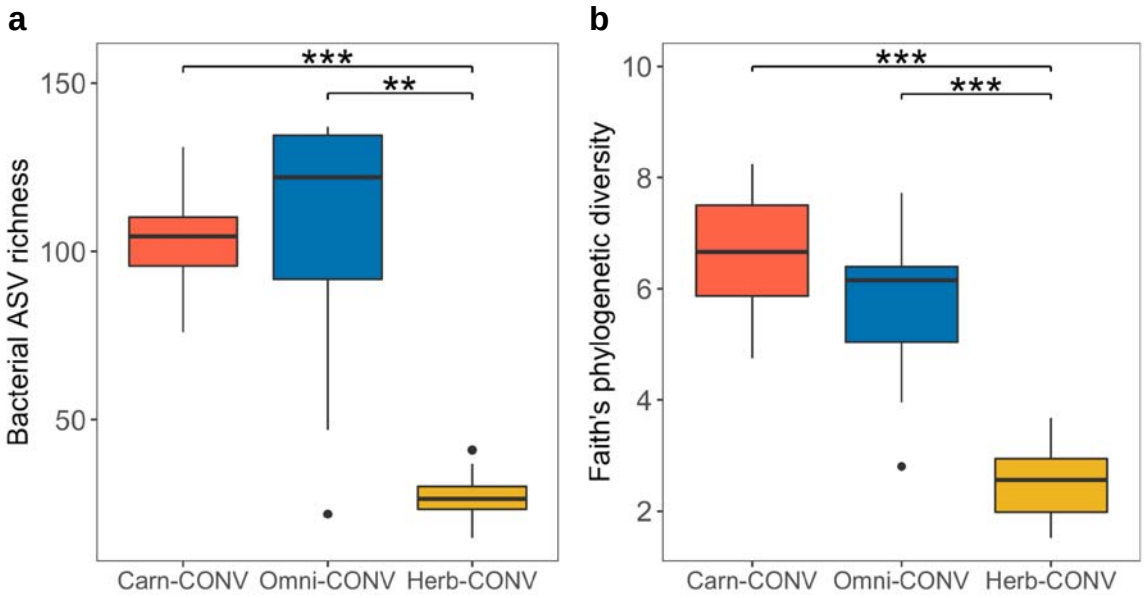

Extended Data Fig. 3. Differences in bacterial alpha diversity across treatment groups. a, Bacterial amplicon sequence variant (ASV) richness differed significantly across treatment groups (F = 16.70, FDR adj. P < 0.001), with Herb-CONV mice exhibiting lower ASV richness compared to Carn-CONV (F = 14.30, P < 0.001) and Omni-CONV mice (F = 10.09, P = 0.002). **b,** Faith's phylogenetic diversity differed significantly across treatment groups (F = 18.50, P < 0.001), with Herb-CONV mice exhibiting lower diversity compared to Carn-CONV (F = 14.29, P < 0.001) and Omni-CONV mice (F = 12.09, P < 0.001). ** denotes P < 0.01 and *** denotes P < 0.001.

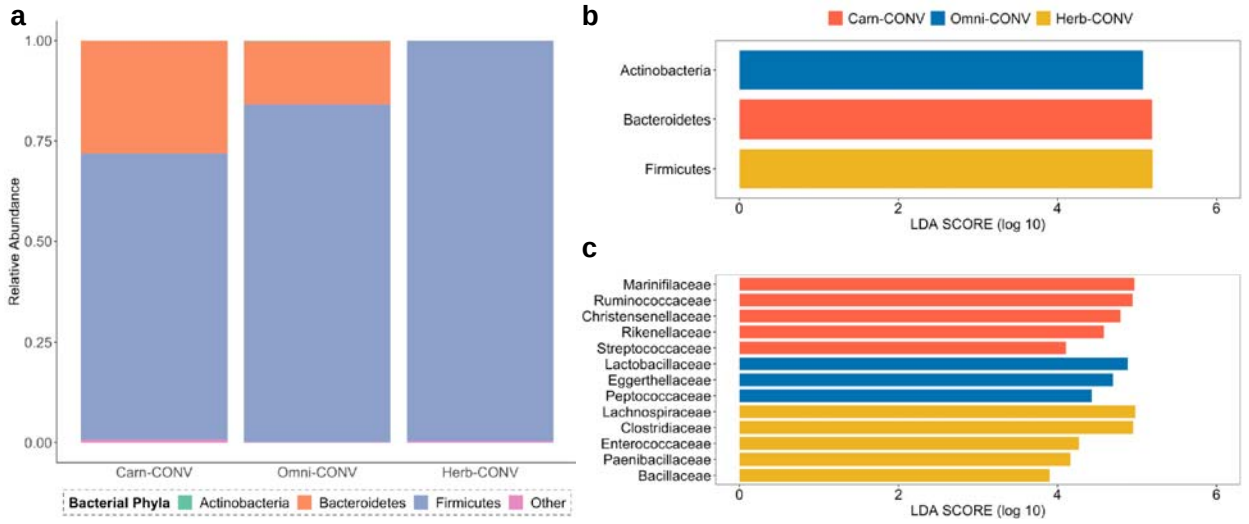

Extended Data Fig. 4. Differences in bacterial community composition across treatment groups. a, Relative abundances of bacterial phyla across treatment groups. **b,** Results of LEfSe analysis showing bacterial phyla that differed significantly in relative abundance across treatment groups. **c,** Results of LEfSe analysis showing bacterial families that differed significantly in relative abundance across treatment groups.

Extended Data Table 1. Nutritional information of HPC and LPC diets.

Diet composition	Low Protein:Carbohydrate diet (LPC)	High Protein:Carbohydrate diet (HPC)
Protein (g/Kg)	140.39	277.44
CHO (g/Kg)	526.23	392.23
Fat (g/Kg)	50.28	49.75
Fiber (g/Kg)	32.90	40.65
NDF (g/Kg)	120.09	119.51
Ca (g/Kg)	9.99	10.01
Cl (g/Kg)	2.77	2.44
K (g/Kg)	8.23	7.72
Mg (g/Kg)	1.67	1.47
Na (g/Kg)	1.36	1.41
P Avail (g/Kg)	3.48	3.47
P (g/Kg)	5.64	5.11
B-12 (mg/Kg)	0.03	0.03
B-6 (mg/Kg)	21.65	20.47
Biotin (mg/Kg)	0.56	0.56
Folic Acid (mg/Kg)	2.36	2.35
Niacin (mg/Kg)	136.36	129.75
Pantothenate (mg/Kg)	68.42	67.71
Riboflavin (mg/Kg)	23.43	23.37
Thiamin (mg/Kg)	19.56	19.84
Vit A (IU/Kg)	19856.00	19888.00
Vit D (IU/Kg)	2204.50	2206.50
Vit E (IU/Kg)	143.92	138.69
Vit K (mg/Kg)	50.07	50.01
Choline (mg/Kg)	2074.46	2045.11
Inositol (mg/Kg)	1128.92	1372.32
PABA (mg/Kg)	110.13	110.13
Vit C (mg/Kg)	991.19	991.19

Extended Data Table 2. Summary of microbiome similarity between conventionalized recipients and their donors. In general, analysis of similarity (ANOSIM) R values indicated that recipient microbiota closely resembled the communities of their donor species. However, equal group beta dispersions (PERMDISP) is a key assumption of ANOSIM, and thus in the cases of Carn-CONV and Herb-CONV conventionalized recipients, the large differences in PERMDISP between treatment groups may render ANOSIM results unreliable. * denotes a q-value (FDR-corrected P-value) ≤ 0.05.

Recipients	Donors	ANOSIM R	ANOSIM q-value	PERMDISP F	PERMDISP q-value
Carn-CONV	*O. torridus*	0.65	0.001*	20.21	0.003*
	M. montanus	1	0.001*	4.09	0.004*
	P. leucopus	0.99	0.001*	4.89	0.01*
Omni-CONV	*P. leucopus*	0.78	0.001*	0.94	0.365
	M. montanus	0.87	0.001*	0.77	0.303
	O. torridus	0.81	0.001*	9.76	0.003*
Herb-CONV	*M. montanus*	0.96	0.001*	8.64	0.003*
	O. torridus	0.9	0.001*	26.49	0.003*
	P. leucopus	0.97	0.001*	9.9	0.003*